

U-Net – based segmentation of *Escherichia coli* cells in the absence and presence of ciprofloxacin exposure

Ozge Umut^{1#}, Miray Esra Palaz^{3#}, Deniz Muratli¹, Aleyna Kizilyer², Sümeyra Vural-Kaymaz^{1,4},
Tugce Ermis¹, Meltem Elitas^{1,4,*}

¹Sabanci University, Istanbul, Turkey

²Istanbul Technical University, Istanbul, Turkey

³Istanbul University, Istanbul, Turkey

⁴Sabanci University Nanotechnology Research and Application Center, Istanbul, Turkey

ABSTRACT

Modern deep learning-based cell segmentation algorithms with high computational power have enabled automated and high-throughput segmentation of bacteria. Previous studies, relying on either manual or automated cell segmentation approaches, have proved that a clonal bacteria population cultured in a regular growth medium in a homogenous microenvironment exhibits heterogeneity. When antibiotic treatment has been applied, heterogeneity of the bacteria population may increase depending on the working mechanisms of an administered antibiotic. Therefore, important features of rare cells, such as asymmetric division of antibiotic persister cells or cells with metastable phenotypes, might be masked by heterogeneity of a population, particularly when a limited number of the cells was analyzed. Therefore, automated image segmentation and analysis approaches have significantly impact on accurate, rapid, and reliable feature identification, particularly for extracting quantitative high-resolution data at high throughput. Here, we implemented U-Net algorithm for segmentation of *Escherichia coli* cells in the absence and presence of ciprofloxacin. The accuracy values were 0.9912 and 0.9869 for the control and ciprofloxacin-treated cell populations, respectively. Next, we developed an algorithm using Python and the OpenCV library to extract the cell number, cellular area, and solidity features of the cells. We believe that our preliminary data might contribute to development of automated, reliable, accurate, and bacteria or antibiotic specific image segmentation tools.

Keywords: Segmentation, *Escherichia coli*, U-Net convolutional networks, Ciprofloxacin, Single-cell analysis, quantification

1. INTRODUCTION

Segmentation of bacteria in crowded and dynamic environments is a complex problem and requires multidisciplinary approach to identify relevant features. For solution, several deep learning-based segmentation algorithms have been developed for automated segmentation of bacteria¹⁻⁶. Although human eye may still be superior for characterizing diverse and arbitrary shaped cell types from imaging data, manually segmenting cells is extremely time-consuming, error-prone, and low throughput¹⁻³. Particularly, when the cells form biofilms or become elongated or branched morphology when they have been exposed to stress conditions such as antibiotics⁴⁻⁶. Recent years several image analysis tools, mostly open-source platforms, for bacteria have been developed to extract cellular features such as cell size, perimeter, elongation rate, growth rate, poles, organelles, trajectories, movement of flagella, while tracking these features over time and relating them to one another in meaningful ways^{3,7}.

Among these powerful and open-source deep learning software, DeepBacs is developed for multi-task bacterial image analysis². DeepBacs uses different deep learning approaches for segmenting bright field and fluorescence time-lapse imaging data of different bacterial species. It classifies growth stages and antibiotic-induced phenotypic alterations. MicrobeJ focused on intensity and morphology measurements of single cells on large image sets. It allows tracking of cells and sub cellular features over time with subpixel resolution³. Cutler and co-workers presented the Omnipose platform, which provides bacteria segmentation in the mixed bacterial cultures, antibiotic-treated conditions, and when the cells have extreme morphological phenotypes⁴. Besides the identification and classification of cellular features or rare cells, tracking bacterial lineages in complex and dynamic environments. Along this line, Bakshi and co-workers used a microfluidic mother machine device for tracking more than 10⁵ parallel cell lineages cultured in the batch conditions⁵. Also, DeLTA,

another CNN-based tool is also developed to track *E. coli* cells in a microfluidic mother machine to perform cell tracking and lineage reconstruction. As DeepBacs, MiSiC is developed as a general deep learning-based 2D segmentation method for high-throughput cell segmentation of complex bacterial communities independent of the microscopy setting and imaging modality⁶. They used a bacterial predator-prey interaction model to analyze bacterial interactions with low computational power. These studies significantly contributed to the field of bacteriology and still requires improved to become fully automated, rapid, easy-to-use, and precise.

Contrary to previous studies, we focus on U-Net based segmentation and quantification of *E. coli* cells in the absence and presence of ciprofloxacin to quantify responses of *E. coli* cells for relatively long time at single cell level for high-throughput analysis¹⁰. We cultured *E. coli* cells on a coverslip with Luria Broth medium in the absence and presence of ciprofloxacin (1.6 $\mu\text{g}/\text{ml}$). Ciprofloxacin is a fluoroquinolone antibiotic that inhibits cell division via inhibiting type II topoisomerase and topoisomerase IV those enroll in DNA separation^{11,12}. Upon ciprofloxacin exposure, *E. coli* cells cannot divide and become elongated¹¹⁻¹³. We acquired the phase-contrast images and implemented the U-Net, a convolutional network that enables high accuracy without requiring large datasets, to segment *E. coli* cells. We used 54 images for both regularly cultured (4761 cells) and ciprofloxacin-treated *E. coli* cells (6005 cells). Next, we developed an algorithm using Python and the OpenCV library to extract the cell number, cellular area, and solidity features of the cells from the segmented data. We believe that our preliminary data might contribute to extraction of quantitative high-resolution information at high throughput for investigating antibiotic responses of bacterial cells. Although, this implementation might seem trivial for the naked eye analysis, high throughput automatic data extraction is a significant computational challenge to detect bacterial cells with different morphologies in the crowded environments.

2. MATERIALS AND METHODS

2.1 Cell Culture and Antibiotic Exposure

We used ATCC 10536 derived *E. coli* K-12 cells from the glycerol stocks. We inoculated it into 2 ml Miller's Luria-Bertani Broth (LB) and incubated at 37°C by shaking at 200 rpm for ~16 h. We used a turbidity at 600 nm absorbance. We dissolved 10 mg of ciprofloxacin (MP Biomedicals™, USA) in 10 ml dimethyl sulfoxide (DMSO) to obtain 10 mg/ml stock solution and stored it at -20 °C. We used the concentrations of 0.16 $\mu\text{g}/\text{ml}$.

Next, we prepared agar pads (1 cm x 1 cm 0.1 cm) using agarose (1.5%) into LB medium. For agar pad containing ciprofloxacin, we add the antibiotic at the final concentration of 0.16 $\mu\text{g}/\text{ml}$ before it solidifies. For the experiments, we grew the cells into early exponential phase (OD_{600nm} = 0.05). Next, we 10-fold concentrated the cells by centrifugation and added 3 μl of the concentrated cell suspension on the agar pad in the absence (control) and presence of ciprofloxacin. Upon loading the cells, we covered the agar pad with a coverslip and incubated the cells on the microscope stage at room temperature for 20 minutes.

2.2 Imaging and Manual Cell Segmentation

Imaging was performed by a Zeiss AxioCam light microscope equipped with a 100x oil immersion objective and a Mrc5 camera. We acquired the phase contrast images every 5 minutes for 5 hours.

Cells were manually segmented using ImageJ both for control data and training data sets. We converted the microscopy images to *tiff* format and cropped to size of 573x537 pixels for the segmentation process. We manually segmented the control group and ciprofloxacin-treated *E. coli* cells using OpenCV library. The masking process includes the conversion of pixels that corresponds cells into white color and the rest of the image into black color. Both groups contain 54 images. Manually segmented images are grouped as training with 50 images and test with 4 images.

2.3 Data Preprocessing and Augmentation

The cropped microscopy images and manually segmented masks reshaped (512,512,3). Then, to augment the dataset, we used the *ImageDataGenerator()* function from the TensorFlow Keras library, applying a range of augmentation methods including rotation (range 0.2), width shift (range 0.05), height shift (range 0.005), shearing (range 0.05), zoom (range 0.05), and horizontal and vertical flip. To ensure that the augmented images were of high quality, we used the nearest fill mode during the augmentation process.

2.4 U-Net Model and Training

We implemented and trained a U-NET model for automated segmentation using some modifications^{10,14}. Specifically, we changed the image format from PNG to TIFF and increased the default input image target size from (256, 256) to (512, 512). The updated U-Net model was trained for 10 epochs, with 2000 steps per epoch for both the ciprofloxacin-treated and control groups separately. The training was performed on a computer with an Intel(R) Core (TM) i9-10900 CPU @ 2.80GHz, 128 GB of RAM, and an NVIDIA RTX A6000 48GB GPU. Each of the training processes took approximately 40 minutes.

2.5 Feature Extraction

When we completed the trainings and tests of the models, we first performed the segmentation and feature extraction using 54 images of the control group. Next, we implemented it to the ciprofloxacin-treated data using 54 images of antibiotic-treated cell population. To extract the features of each cell from the resulting masks, we developed a custom algorithm using the OpenCV library. In this algorithm, we first applied binary thresholding to the masks using the `cv::threshold()` function. The threshold and the max value parameters of the function were set to 150 and 255, respectively. Consequently, the pixel values smaller than 150 were mapped to 0 (black) and those greater and equal to 150 to 25 were mapped to 255 (white). Afterwards, we used the `cv::findContours()` function with simple chain approximation to detect the contours of the cells. We extracted the area and perimeter features from each contour using the `cv::contourArea()` and `cv::arcLength()` functions, respectively. Additionally, we calculated the solidity of each cell, which can be calculated as the ratio of the total area to the convex hull area¹⁰. The convex hull area of a group of points is defined as the area of the smallest convex polygon enclosing all these points. In our case, the convex hull area of a cell was the area of the smallest convex polygon that completely encloses the cell. We determined these polygons using the `cv::convexHull()` function and calculated their area similarly to calculation of the cellular area. After extracting the features of each cell for each image, we computed their average, minimum, maximum, and standard deviation values.

3. RESULTS

We implemented U-Net algorithm for segmentation of *E. coli* cells in the absence and presence of ciprofloxacin. First, we cultured *E. coli* cells in the test tubes, and we prepared the agar pads, as explained above. Next, we sandwiched the cells between an agar pad and a cover slip, then acquired phase-contrast images of the cells, Figure 1.

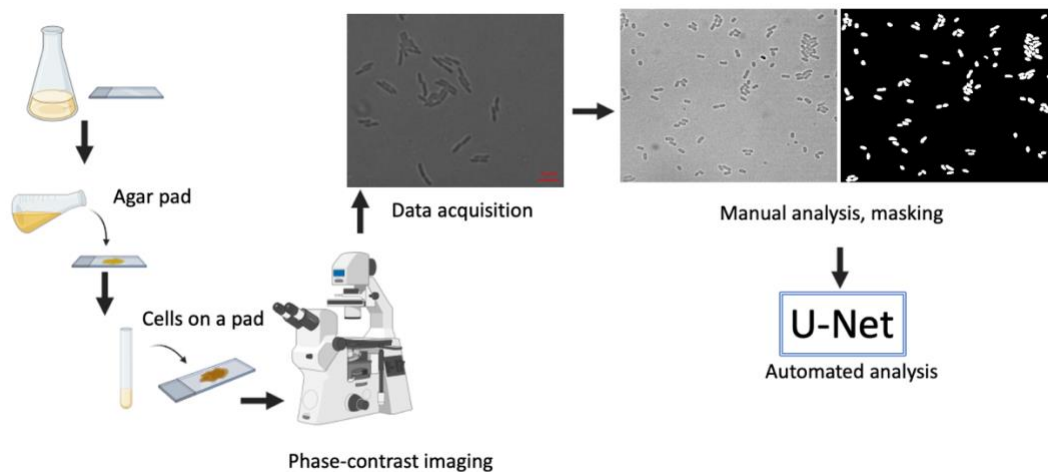


Figure 1. Experiment plan. The scale bar is 5 μm .

When we trained the U-Net model for the *E. coli* cells in the control group, we obtained 1.62 % loss and 99.28% accuracy values. These values were 2.88 % loss and 98.69 % accuracy for the *E. coli* cells in the ciprofloxacin-treated group.

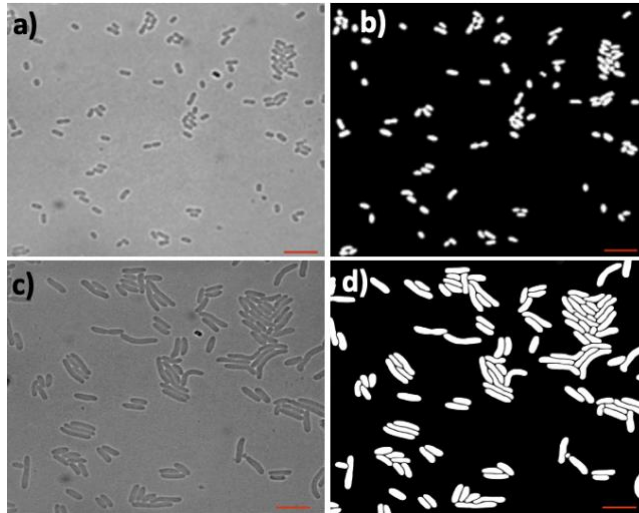


Figure 2. U-Net implementation for *E. coli* cells for the control group a) original image, b) segmented cells, for the ciprofloxacin-exposed group c) original image, d) segmented image. The scale bar is 5 μm .

Table 1 summarizes the number of the *E. coli* cells that were counted by our custom algorithm using OpenCV from masks automatically generated by U-Net and by Fiji using manually segmented masks.

Table 1. Comparison of cell numbers in the control and antibiotic-treated cell cultures using U-Net predicted masks and custom algorithm and using manually segmented masks and Fiji.

	Control cells	Ciprofloxacin-treated cells
<i># of cells by Fiji</i>	4531	6154
<i># of cells by OpenCv</i>	4761	6005
<i>Loss</i>	0.0162	0.0288
<i>Accuracy</i>	0.9928	0.9869

We calculated the average area, perimeter, and solidity features by our algorithm for the control group and ciprofloxacin-treated *E. coli* cells. Figure 3 illustrates the distribution of these features for each frame and the statistical differences between the control and antibiotic-treated groups. We observed that ciprofloxacin hinders the cell division process, leading to the elongation of cells and an increase in cellular area and perimeter measurements. We obtained consistent results between manually and automated cell segmentation results, Table 1.

Next, using the U-NET data we compared the changes in the cellular area and perimeters of the cells in the absence (black circles) and in the presence of ciprofloxacin (blue squares), Figure 3a-3f. Since these cells were elongated in the presence of ciprofloxacin, there was a significant difference for the area and perimeter measurements ($p < 0.0001$). Besides, heterogeneity of the cells was increased when they were treated with ciprofloxacin, Figure 3b, 3d. The average cellular area and perimeter were 151.6 pixel^2 , 65.63 pixel for the control group cells, respectively. In terms of solidity, we did not observe a clear pattern. Initially, the solidity values of the ciprofloxacin-treated culture were slightly higher than the control group. However, the solidity value of the control group became slightly higher in the last 11 frames, Figure 3e. Although there was not statistically significant difference between these groups ($p: 0.7830$), there were two subpopulations in terms of solidity both in the control and antibiotic-treated groups, Figure 3f.

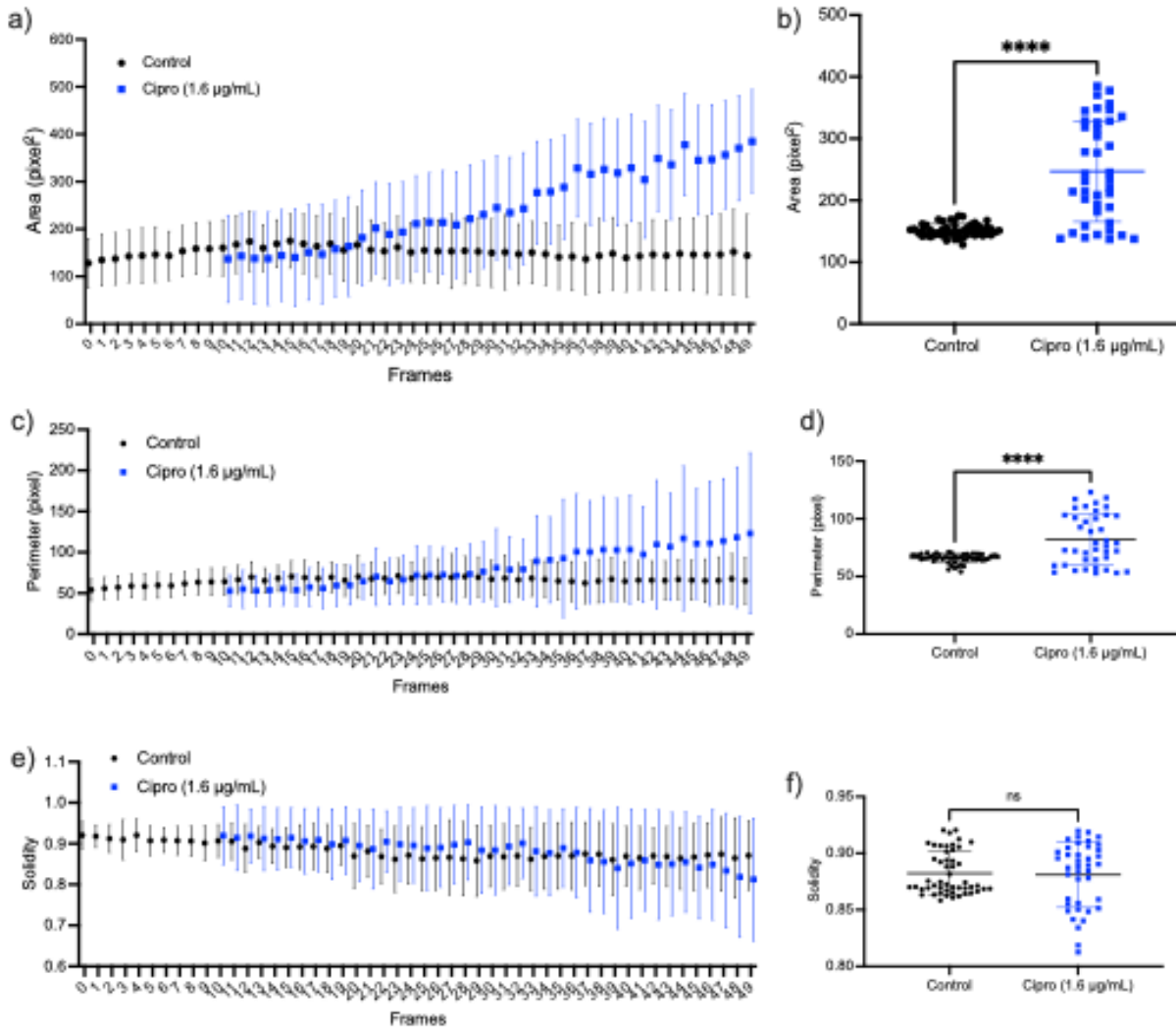


Figure 3. Distribution of cellular properties and statistical comparison of control group and antibiotic-treated group pf cells. a) Distribution of cellular area, b) Area comparison, c) Distribution of perimeters of the cells, d) Perimeter comparison, e) Distribution of solidity, f) comparison of solidity. ns: not statistically significant, **** > 0.0001 .

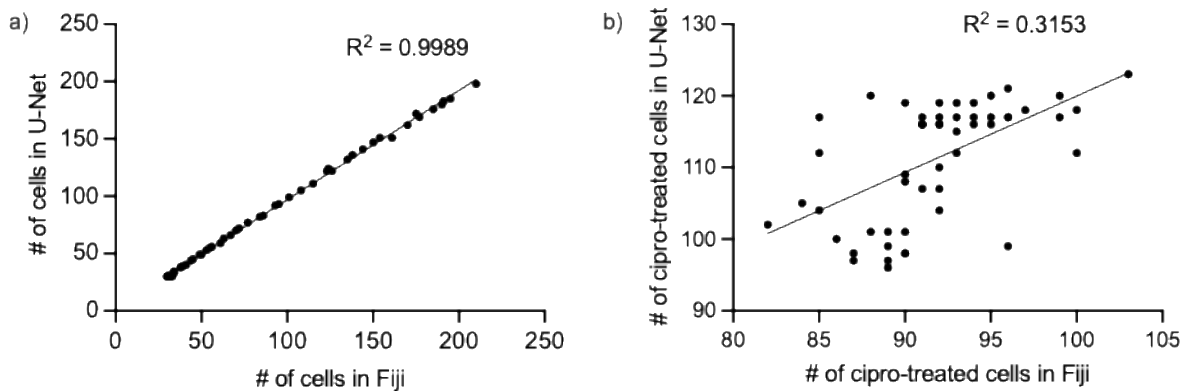


Figure 4. Comparison of U-Net and Fiji cell counting

Our simple linear regression test showed that U-Net-based obtained data fits well with the manually counted cell data for the antibiotic-free culture ($R^2 = 0.9989$), Figure 4a. On the other hand, we could not obtain a similar performance for the

antibiotic treated cell population, ($R^2 = 0.3153$), Figure 4b. To solve this problem, hyperparameter tuning can be applied to the U-Net model to improve the generated masks. Also, Fiji program or the `cv::findContours()` function from OpenCV library might have problems to find contours of elongated cells or clustered cells.

4. CONCLUSION

In this paper, we presented the employment of U-Net – based cell segmentation algorithm for *E. coli* cells in both regular growth and ciprofloxacin treatment conditions. Our results provided 0.9912 and 0.9869 accuracy values for the control and ciprofloxacin-treated cell populations, respectively. Our further work will focus on increasing the number of analyzed images. Next, we will perform this analysis for different types of antibiotics which causes cell death based on different killing mechanisms. Our main goal is to generate a framework that can identify and segment different types of bacteria, in the absence and presence of various antibiotics. Finally, clinically important properties of the cells can be accurately obtained and rapidly reported to medical person.

REFERENCES

- [1] Jeckel, H., Drescher, K., “Advances and opportunities in image analysis of bacterial cells and communities,” FEMS Microbiology Reviews, fuaa062, 45, 1-14 (2021).
- [2] Spahn, C., Gómez-de-Mariscal, E., Laine, R. F., Pereira, P. M., von Chamier, L., Pinho, M. G., Jacquement, G., Holden, S., Heilemann, M., Henriques, R., “DeepBacs for multi-task bacterial image analysis using open-source deep learning approaches,” Communications Biology, 5, 688 (2022).
- [3] Ducret, A., Quardokus, E. M., Brun, Y. V., “MicrobeJ, a tool for high throughput bacterial cell detection and quantification,” Nature Microbiology, 1, 16077 (2016).
- [4] Culter, K. J., Stringer, C., Lo, T. W., Rappez, L., Stroustrup, N., Peterson, S. B., Wiggings, P. A., Mougous, J. D., “Omnipose: a high-precision morphology-independent solution for bacterial cell segmentation,” Nature Methods, 19, 1438-1448 (2022).
- [5] Kysela, D. T., Randich, A. M., Caccamo, P. D. & Brun, Y. V., “Diversity takes shape: understanding the mechanistic and adaptive basis of bacterial morphology,” PLoS Biol. 14, e1002565 (2016).
- [6] Bakshi, S., Leoncini, E., Baker, C., Cañas-Duarte, S. J., Okumus, B., Paulsson, J., “Tracking bacterial lineages in complex and dynamic environments with applications for growth control and persistence,” Nature Microbiology, 6, 783-791 (2021).
- [7] Scheider, C.A., Rasband, W.S., Eliceiri, K. W., “NIH image to ImageJ: 25 years of image analysis,” Nature Methods, 9, 671-675 (2012).
- [8] Panigrahi, S., Murat, D., Le Gall, A., Martineau, E., Goldlust, K., Diche, J.-B., Romboust, S., Nollman, M., Espinosa, L., Mignot, T., “MiSiC, a general deep learning-based method for the high-throughput cell segmentation of complex bacterial communities,” eLife Sciences 10 (2021).
- [9] Lugagne, J.-B., Lin, H., Dunlop, M. J., “DeLTA: Automated cell segmentation, tracking, and lineage reconstruction using deep learning,” PLoS Comput Biol, 16, e1007673 (2020).
- [10] Falk, T., Mai, D., Bensch, R. et al., “U-Net: deep learning for cell counting, detection, and morphometry,” Nat Methods 16, 67–70 (2019).
- [11] Elliott, T. S. J., Shelton, A., Greenwood, D., “The response of Escherichia coli to ciprofloxacin and norfloxacin,” J. Med. Microbiol., 23, 83-88, (1987).
- [12] Mason, D. J., Power, E. G., Talsania, H., Phillips, I., Gant, V.A., “Antibacterial action of ciprofloxacin,” Antimicrobial Agents and Chemotherapy, 39(12), 2752-2758 (1995).
- [13] Ponmalar, I. I., Swain, J., Basu, J. K., “Modification of bacterial cell membrane dynamics and morphology upon exposure to sub inhibitory concentrations of ciprofolaxcin,” Biomembranes, 183935 (2022).
- [14] <https://github.com/zhixuhao/unet>